

SUSY- $\tilde{e}^\pm/\tilde{\mu}^\pm$ Studies

LCWS-2000 talk, October 2000 - Fermilab
COLO-HEP-454

M. Dima, dima@pizero.colorado.edu
Dept. of Physics, Campus Box-390,
Colorado University - Boulder,
CO-80309, USA

The $e^+e^- \rightarrow \tilde{l}^+ \tilde{l}^-$ mode has the discovery potential for SUSY-leptons and allows the determination of the LSP and SUSY-lepton masses. This study looks at the practical issues regarding the mode, such as background rejection, efficiency of cuts, both in the classical and neural network approaches.

In supporting the physics programme for the Next Linear Collider [1] (NLC) thorough investigations of reaction modes, backgrounds, as well as detector response, CPU usage, *etc* are conducted in order to evaluate the NLC discovery potential for Supersymmetry [2] (SUSY), or other new physics.

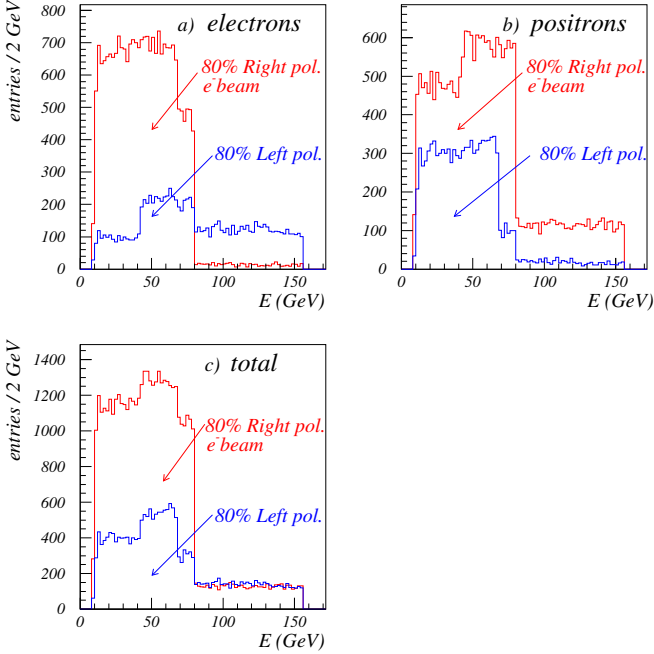


FIG. 1. Energy distributions for signal tracks visible in the event: a) electrons, b) positrons and c) both. The changes in the distributions with the switch of the e^- beam polarization are due to the $\tilde{l}_{L/R}^\pm$ production rate variation with beam polarization and are unique to SUSY. No Standard Model (SM) signal has any similar behavior.

An important reaction mode for the discovery of SUSY-particles is $e^+e^- \rightarrow \tilde{l}^+ \tilde{l}^-$ where the SUSY-leptons decay to the Lightest Supersymmetric Particle (LSP) $\tilde{l}^\pm \rightarrow \tilde{\chi}_1^0 l^\pm$. The mode is characterized by energy “box distributions” of the visible particles in the detector, figure 1 - simulated signal from SUSY Point-2: $m_0 = 100 \text{ GeV}/c^2$, $m_{1/2} = 300 \text{ GeV}/c^2$, $A_0 = 0$, $\tan\beta = 2$, $\mu = -550$, $m_{\tilde{e}_L^\pm} = 238 \text{ GeV}/c^2$, $m_{\tilde{e}_R^\pm} = 157 \text{ GeV}/c^2$ and $m_{\tilde{\chi}_1^0} = 128 \text{ GeV}/c^2$. The flat distribution is due to the boost of the l^\pm CMS angular distribution into the LAB system of reference: $E_{LAB} = \gamma(E_{CMS} + \vec{\beta} \cdot \vec{p}_{CMS})$. The magnitude of the boost is constant, and so are the CMS quantities (in both cases dictated by two body decay kinematics), however the helicity angle distribution (CMS l^\pm -angle with respect to boost direction) is not always flat. In the present case a spin-0 particle decays to two fermions, the final state particles being in an S-wave ($L = 0$, flat angular distribution). As a consequence, the

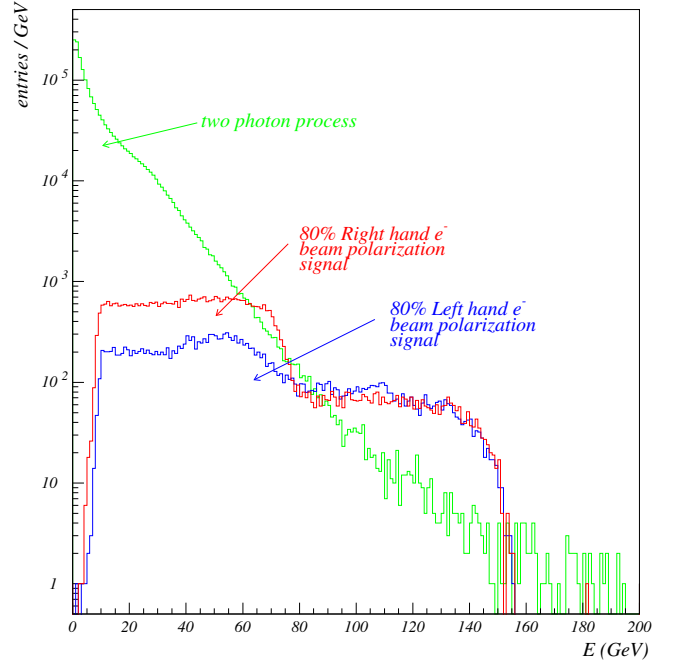


FIG. 2. Energy distribution of particles visible in the detector for the two photon process (green) and signal: (blue) for 80% Left, respectively (red) for 80% Right hand polarized, e^- beam polarization signal, all on logarithmic scale.

E_{LAB} distribution is also flat. Conversely, the E_{LAB} distribution can be a check for the angular distribution in the CMS, and used to confirm the spin of the particles involved. The edge positions of the distribution are uniquely determined by the masses of the particles in the reaction, and can be used to determine these masses.

The visible signal in the detector are two lepton tracks. The tracks were run through the GEANT 3.0 [3] detector simulation. The masking of the signal by SM events has been studied elsewhere [4] and cuts were optimised. A background whose magnitude was realised later in the analysis by N. Danielson, U. Nauenberg and D. Wagner is the two photon process [5]. These events involve two virtual photons ($\gamma^*\gamma^*$) producing an $l^+ l^-$ pair and give rise to a background 2-3 orders of magnitude higher than that of the SUSY signal, figure 2. Using a 3 year's worth of ISAJET [6] simulated signal, an equal running time sample of two photon background events was compared to the SUSY signal, for the machine running at $\sqrt{s} = 500$ GeV. Figure 3 shows the $(p_{\perp}^{min}, p_{\perp}^{max})$ distribution for background (green) and signal: (blue) - for 80% Left, and (red, with p_{\perp}^{min} and p_{\perp}^{max} interchanged) - 80% Right hand e^- beam polarization. Min/max refers to the lower/higher p_{\perp} track in the event. It is evident

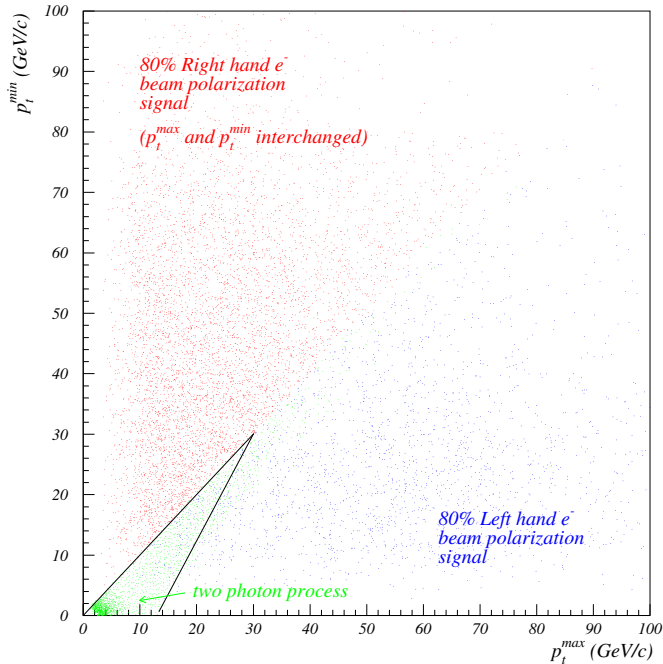


FIG. 3. Distribution of $(p_{\perp}^{min}, p_{\perp}^{max})$ for the two photon process (green) and signal: 80%-Left (blue, lower diagonal) and 80%-Right hand e^- beam polarization signal (red, upper diagonal with p_{\perp}^{min} and p_{\perp}^{max} interchanged). The two photon process is mostly concentrated in the 2-6 GeV/c region and can be eliminated to a large extent by the “wedge”-cut illustrated. The primary high energy $e^+ e^-$ of the two photon process are scattered within 40 mrad of the beam line.

that for $m_{\tilde{l}_{R/L}} - m_{\tilde{\chi}_1^0} = 30/110$ GeV c^{-2} (our present case) the signal region has only some overlap with the background. However, when $m_{\tilde{l}_{R/L}} \simeq m_{\tilde{\chi}_1^0}$ (“degenerate” case), $p_{\perp}^{min} \simeq p_{\perp}^{max} \simeq 0$ and the signal “shrinks” into the area occupied by the two photon process. A “wedge” cut was applied to eliminate the two photon process, as shown by the contour in figure 3. This reduces the background to the same order of magnitude as the signal. To further suppress the two photon process the missing p_{\perp} in the event (p_{\perp}^{event}) was considered for signal and background, figure 4. The two photon process after the “wedge” cut” peaks as a gaussian in the lower p_{\perp}^{event} region, a cut being applied as shown in figure 4 to completely eliminate this background. The combined efficiency of the two cuts is 94 % (for Left), respectively 86 % (for Right hand e^- beam polarization). The signal before and after cuts, including the two photon process (6 events) is shown in figure 5. It is important to note that the cuts preserve the edges of the distribution, needed

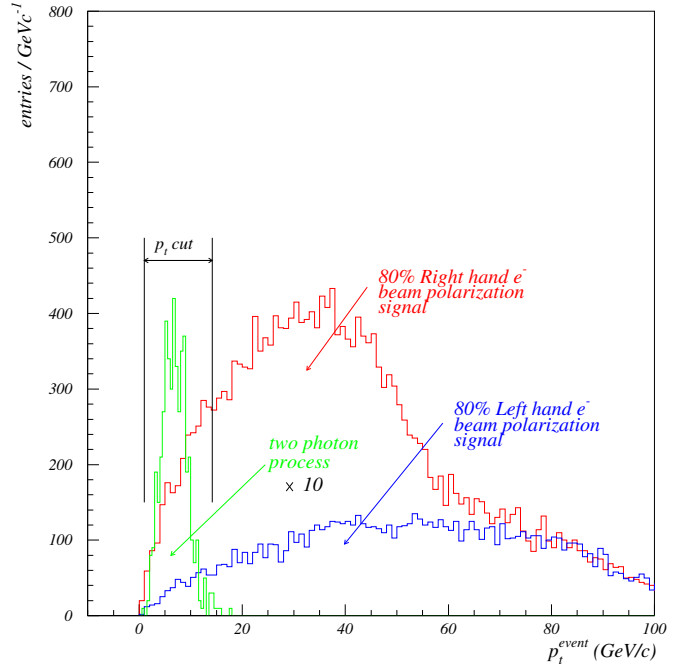


FIG. 4. Distribution of p_{\perp}^{event} for the two photon process (green - $\times 10$) and 80%-Left (blue), respectively 80%-Right hand e^- beam polarization signal (red). The p_{\perp}^{event} cut featured eliminates entirely the two photon background.

to determine the masses of the supersymmetric particles. These results are very encouraging, however the selection criteria must be evaluated against the present understanding of both signal and background. To compensate for the limited understanding of the two photon signal, the “wedge” cut featured in figure 3 has to be widened. This is particularly damaging to the signal in the degenerate case when the signal “shrinks” into the area occupied by the two photon signal. To avoid

this problem additional combinations of parameters with similar selection power were sought. Should such combinations exist, they would be manifest in the performance of an Artificial Neural Network [7] (ANN). A Multi-Layer Perceptron [8] (MLP) was trained for different configurations of input variables, its training error as a function of the training “epoch” being shown in figure 6 for one of the input variable configurations. The point at which the error on the “independent” sample exceeds that of the “training” sample is the *overtraining* threshold. At this point the training is stopped and the MLP “pruned”, *i.e.* - the weaker links in the ANN are removed. Pruning is performed in order to avoid local minima in the

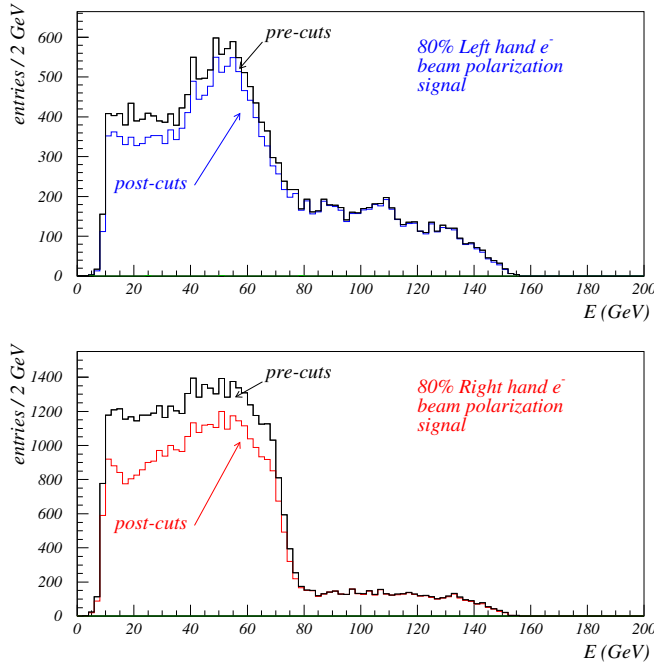


FIG. 5. Comparison of signal pre- and post-cuts, (blue) for 80% Left and (red) for 80% Right hand polarized e^- beam. This includes the 6 two photon events remaining after the cuts. The cuts do not deteriorate the edges of the signal distribution, which is essential for determining the SUSY particle masses. The bolding of the distribution’s high edge is due to the Calorimeter and is presently under investigation.

training process. Training¹ is then resumed until the MLP is once more close to overtraining. At this point the neural links in the MLP are not a function of the training history and the best response has been attained. The output of the MLP should ideally be 0 for background

¹BFGS quadratic training method (Broyden, Fletcher, Goldfarb and Shanno), method that approximates the inverse of the Hessian matrix iteratively. Efficient, however memory intensive.

and 1 for signal events, however in practice a distribution is observed, as shown by figure 7. A cut at 0.8 was made in order to delimit the signal from the background, any output smaller than 0.8 being considered “background”. The results with the ANN-based selection however did not exceed the performance of the analytical method, indicating the absence of additional “exotic” parameters with potentially effective cuts. The question arises what is the degeneracy limit $\Delta M_{SUSY}^{R/L} = m_{\tilde{l}_{R/L}^\pm} - m_{\tilde{\chi}_1^0}$ down to which the present method can still discern the signal from background.

To eliminate the total dependence on the above cuts, a Čerenkov Detector [9], housed in the beampipe - with acceptance down to $\theta \simeq 20$ -30 mrad, was proposed for the detection of the scattered high-energy e^+ and e^- in two photon events. This would constitute a “hardware” confirmation of the event as a background event, avoiding

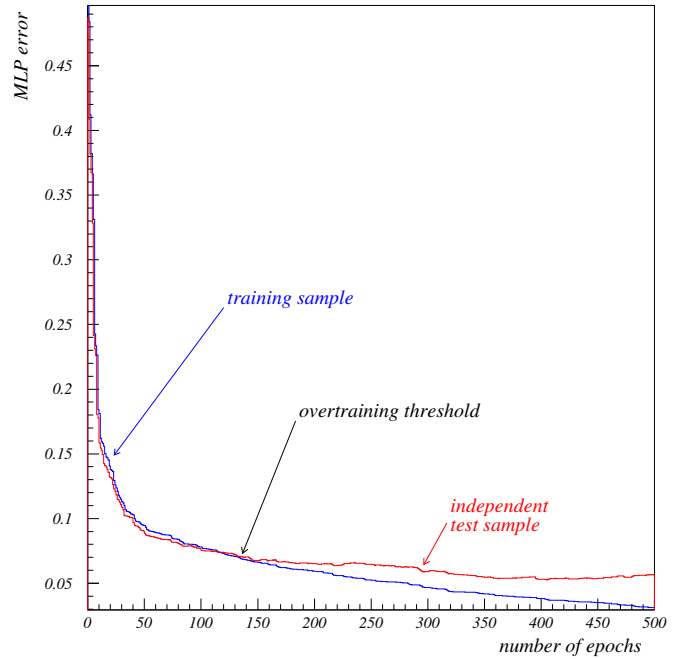


FIG. 6. MLP training error for the “training” sample (blue) and for the “independent” test-sample (red). “Overtraining” occurs after approximately 150 epochs.

the previous method’s uncertainties. Figure 8 shows the distribution of two photon events as containment angle *vs.* p_\perp^{event} . It can be seen that most two photon events lie in the range of 12-17 mrad, with the tail extending beyond 40 mrad (within the actual detector’s acceptance). As it can be seen from figure 8, for lower θ the Čerenkov Detector has to be augmented by a cut on p_\perp^{event} . A Čerenkov Detector going down to $\theta \simeq 30$ mrad, requires an additional p_\perp^{event} cut at 7.3 GeV/c, respectively one to $\theta \simeq 20$ mrad, a cut at $p_\perp^{event} > 5$ GeV/c. The effect of the cuts on the signal is shown in the lower plot in figure

8. For a far from “degenerate” case, $\Delta M_{SUSY}^{R/L} = 30/110 \text{ GeVc}^{-2}$, the cuts remove little signal, however as the signal comes from a more degenerate case, the distribution contracts towards zero and the effect of the cuts is more damaging. Establishing a “visibility” limit for this technique is currently under detailed investigation.

The present contribution has shown the results of the SUSY- $\tilde{e}^\pm/\tilde{\mu}^\pm$ analysis in the context of GEANT-3.0 simulated detector response. Highly effective cuts against the huge expected two photon process were designed, both in the classical (analytical), as well as in the Neural Network approach. It was shown that the signal cannot be discerned from background in the “degenerate” case, when $m_{\tilde{t}^\pm_{R/L}}$ and $m_{\tilde{\chi}_1^0}$ differ by a very small amount. The

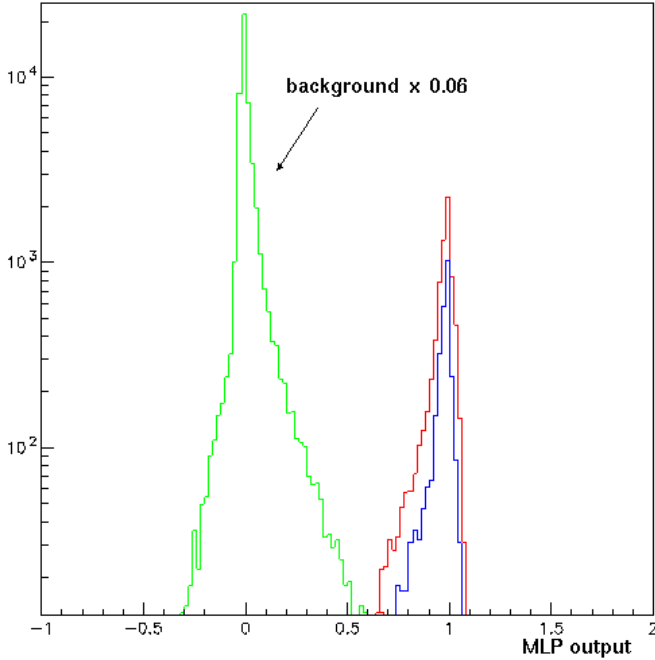


FIG. 7. MLP output on a log-scale for two photon events (green) and signal: 80% Left (blue), respectively 80% Right hand e^- beam polarization signal (red). The MLP’s output is the product of 2 neural “nodules”, trained separately to select Left/Right hand signal. A cut at 0.8 was placed to eliminate the background, the rejection factor being 7500:1. The signal efficiencies of the cut are 86% for both Left and Right hand polarizations.

limit down to which the analysis can go is enhanced by a Čerenkov detector housed in the beampipe, with an angular acceptance of 20 mrad.

I would like to thank the students at the University of Colorado - Boulder working on the NLC Project for running the ISAJET and GEANT simulations and providing the data in a friendly processable format. We acknowledge support for this work under DOE grant DEFG03-95ER-40894.

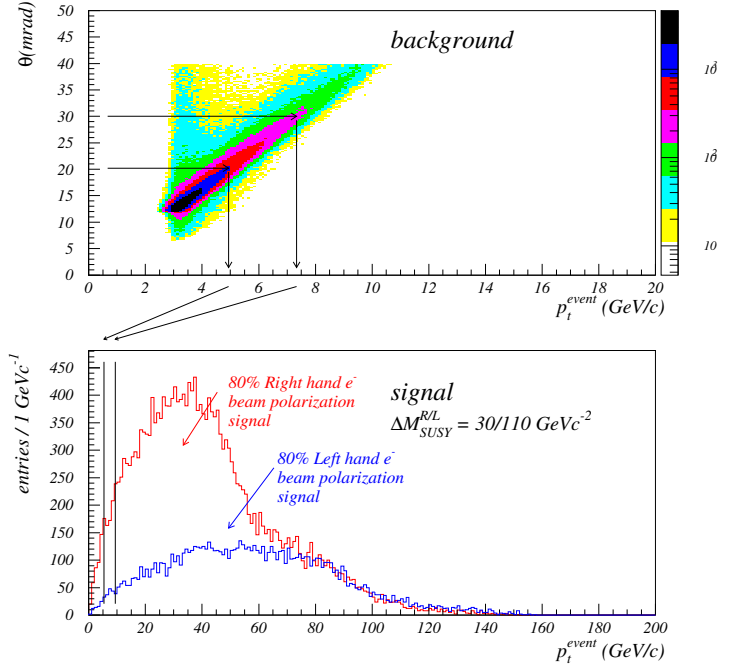


FIG. 8. Containment angle of the scattered high energy e^+ and e^- from two photon events versus p_{\perp}^{event} . The $\gamma^*\gamma^*$ background can be eliminated with a Čerenkov Detector installed down to 20 mrad acceptance. For lower θ , the detector needs to be augmented by a p_{\perp}^{event} cut. The effect of the latter cut on the signal is shown in the lower plot. The chart colors are yellow for above 10^1 , green for 10^2 and blue for 10^3 .

- [1] *Physics and Technology of the Next Linear Collider*, BNL 52-502, Fermilab-PUB-96/112, LBNL-PUB-5425, SLAC Report 485, UCRL-ID-12416.
- [2] H.P. Nilles, *Phys. Repts.* **110**, 1 (1984); H. Haber and G. Kane, *Phys. Repts.* **117**, 75 (1985); H. Murayama in *Physics with High Energy Colliders*, S. Yamada and T. Ishii, eds. (World Scientific, Singapore, 1995); M.E. Peskin, *Prog. Theor. Phys. Suppl.* **123**, 507 (1996).
- [3] GEANT-3.0, CERNLIB software, R. Brun, M. Hansroul and J.C. Lassalle. *GEANT User's Guide* (1982).
- [4] E. Goodman, COLO-HEP-398, (1998).
- [5] N. Danielson, COLO-HEP-423, (1998).
- [6] *ISAJET 7.51, A Monte Carlo Event Generator for pp, p-pbar and e+ e- Reaction*, F.E. Paige, S.D. Protopopescu, H. Baer and X. Tata, (2000).
- [7] B. Denby, *Comput. Phys. Commun.* **119**, 219 (1999); H. Robbins and S. Monro, *Ann. Math Stat.* **22**, 400 (1951).
- [8] J. Schwindling and B. Mansoulié, MLPfit 1.40 package, CERNLIB (1999).
- [9] J. Barron, COLO-HEP-449, (2000); C.S. Takeuchi and R.C. Kelly, COLO-HEP-450 (1999).